

NUCLEON-NUCLEON INTERACTION AT AN ENERGY OF 9 Bev

I. M. GRAMENITSKII, I. M. DREMIN, V. M. MAKSIMENKO, and D. S. CHERNAVSKII

P. N. Lebedev Physics Institute, Academy of Sciences, U.S.S.R.

Submitted to JETP editor September 21, 1960

J. Exptl. Theoret. Phys. (U.S.S.R.) 40, 1093-1100 (April, 1961)

The pole approximation<sup>3,4</sup> is employed to describe peripheral collisions of nucleons at 9 Bev. The results of the calculations are compared with the experimental data,<sup>1,2</sup> and the agreement is found to be satisfactory. The region of applicability of the pole approximation is estimated and the possibility of obtaining information on the properties of the  $\pi$ -meson propagation function and  $\pi N$  interaction cross section as a function of the square of the  $\pi$ -meson 4-momentum ( $k^2$ ) is discussed.

INTRODUCTION

AN abundance of experimental data on the nucleon-nucleon (hereafter, NN) interaction at an energy of 9 Bev is now available.<sup>1,2</sup> On the other hand, the recently suggested pole method of calculating strong interactions has been further developed.<sup>3-5</sup> It is therefore of interest to compare the theoretical data on the NN interaction at 9 Bev with the experimental data.

It should be noted that certain experimental data<sup>1,2</sup> (for example, the strongly anisotropic c.m.s. angular distribution of the nucleons, the c.m.s. asymmetry of charged particles, etc.) directly indicate the important role of peripheral interactions in this process. One can state in advance that these data cannot be explained with the aid of the statistical theory<sup>6-8</sup> of central nucleon-nucleon collisions.

METHOD

We shall not consider here all the aspects of the pole method, which has been described in detail in references 3 - 5; we shall discuss only the assumptions on which it is based.

1. The propagation function of the intermediate meson in the general case should have the form

$$D(k^2) = \frac{1}{k^2 + \mu^2} + \int_{(3\mu)^2}^{\infty} \frac{\rho(x)}{k^2 + x} dx, \tag{1}$$

where  $\rho(x)$  is an essentially positive function which is not yet known;  $k$  is the 4-momentum of the intermediate meson,  $k^2 = k^2 - k_0^2$ ,  $\hbar = c = 1$ ;  $\mu$  is the  $\pi$ -meson mass. In the one-meson pole approximation, only the first (pole) term in expression (1) is taken into account; it is seen from (1) that the influence of the second term is important only for  $k^2 \geq (3\mu)^2$ .

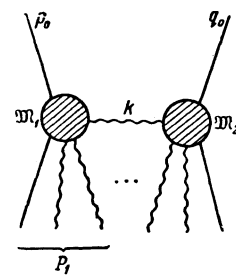


FIG. 1.

2. The cross section for the interaction between a  $\pi$ -meson and a nucleon depends on the energy  $\omega$  (in the c.m.s. of the nucleon and  $\pi$  meson) and also (if the  $\pi$  meson is virtual) on the quantity  $k^2$ . In the general case, we can write

$$\sigma(\omega, k^2) = \sigma(\omega, k^2 = -\mu^2) - \Sigma(\omega, k^2). \tag{2}$$

The first term represents here the cross section for the interaction between a real  $\pi$  meson ( $k^2 = -\mu^2$ ) of energy  $\omega$  and a nucleon. The role of the second term has not yet been investigated in detail.\* It, too, is neglected in the pole method.

3. Only the one-meson diagram is considered in the pole method (Fig. 1). Diagrams in which the nucleons exchange two, three, etc. mesons are not considered. The basic question that arises in the estimate of the permissibility of this simplification is not the extent of contribution to the cross section, but whether there is significant interference between the one-meson diagram and the multi-meson diagrams. In fact, if the interference is not significant, then the contributions of the various diagrams to the cross section are additive; the

\*Generally speaking, the sign of the second term cannot be determined beforehand. It is very likely to be negative [i.e.  $\sigma(k^2)$  decreases with an increase in  $k^2$ ].

calculation of the one-meson diagram is of value in itself, and can be used to describe part of the experimental data. The question of interference is complicated and merits special investigation. We present here only a number of arguments indicating that this effect plays an unimportant role.

In the case of the one-meson exchange, two groups of particles are produced from nodes 1 and 2. These groups of particles have anisotropic distributions (in the c.m.s.) and are emitted in different directions. The greatest interference between the one-meson matrix element and the two-meson (in general, multi-meson) matrix element occurs when the angular distributions are similar.

In this case, however, interference will occur only if all the quantum numbers characterizing each group of particles [the intrinsic angular momentum (spin)  $J$ , its projection on any axis  $m_y$ , the parity  $I$ , the isotopic spin  $T$ , etc.] coincide. In the case of exchange of one meson,  $T = \frac{1}{2}, \frac{3}{2}$ ;  $m_y = \frac{1}{2}$ . (Here  $m_y$  is the projection of the spin on the momentum of the primary nucleon in the system in which the momentum of the entire group of particles is zero.) If it is assumed that the quantities  $T$ ,  $T_z$ , and  $m_y$  in multi-meson exchange are distributed at random, then one can estimate the probability that they all coincide with the corresponding quantities for one-meson exchange. For the two-meson exchange, the requirement that only the quantities  $T$ ,  $T_z$ , and  $m_y$  coincide leads to the probability  $W \sim 0.1$ . The requirement that all other quantities coincide (total angular momentum  $J$  and parity  $I$ ) can only reduce this estimate.

Using the three assumptions enumerated above, we can write an expression for the inelastic NN-interaction cross section:

$$\sigma_{NN}(E_0) = \frac{2}{(2\pi)^3 p_0^2 E_0^2} \int dz dy \sqrt{z^2 - m^2} \sqrt{y^2 - m^2} + \left\{ \frac{1}{\mu^2 + \kappa^2} - \frac{1}{\mu^2 + \kappa^2 + 4p_0 p_1} \right\} \times \begin{cases} \frac{10}{9} \sigma_{3/2}(z) \sigma_{3/2}(y) + \frac{16}{9} \sigma_{3/2}(z) \sigma_{1/2}(y) + \frac{1}{9} \sigma_{1/2}(z) \sigma_{1/2}(y) \text{ for } pp \\ \frac{14}{9} \sigma_{3/2}(z) \sigma_{3/2}(y) + \frac{8}{9} \sigma_{3/2}(z) \sigma_{1/2}(y) + \frac{5}{9} \sigma_{1/2}(z) \sigma_{1/2}(y) \text{ for } pn \end{cases}$$

Here

$$z = \frac{1}{2} (\mathfrak{M}_1^2 - m^2 - \mu^2), \quad y = \frac{1}{2} (\mathfrak{M}_2^2 - m^2 - \mu^2), \quad (3)$$

$\sigma_{3/2}(z)$  is the cross section for the interaction between a  $\pi$  meson and nucleon at an energy  $\omega_L = z/m$  in the isospin state  $\frac{3}{2}$  etc.;  $\kappa^2 = 2(E_0 E_1 - p_0 P_1) - \mathfrak{M}_1^2 - m^2$  (the quantity  $\kappa^2$  reflects the virtualness of the  $\pi$  meson and is of the order of magnitude  $k^2/2$ );  $E_0$ ,  $p_0$ , and  $m$  are the c.m.s. energy, momentum, and mass of the primary nucleon;  $E_1$  and  $p_1$  are the energy and momentum

of the entire group of particles emitted from node 1;  $\mathfrak{M}_1 = \sqrt{E_1^2 - P_1^2}$  is the energy of this group of particles in its rest system;  $E_2$ ,  $P_2$  and  $\mathfrak{M}_2$  are the corresponding quantities for node 2.

Hereafter, for convenience, we shall call these groups of particles isobars and carry out the calculations in two steps: a) the calculation of the production of the two isobars (with masses  $\mathfrak{M}_1$  and  $\mathfrak{M}_2$ ) and b) their decay into secondary particles. This procedure is used primarily to facilitate the calculations, but it is also justified physically, since the time for the production of the isobars, as a rule, is much smaller than the time for their decay. In fact, the production of an excited state is a one-quantum process, and its time in the rest system of the isobar is estimated from the uncertainty relation  $\tau_1 \Delta E \sim \hbar$  ( $\Delta E$  is the excitation energy). The decay of the excited state is a multi-quantum classical process and the time for it is  $\tau_2 \Delta E \gg \hbar$ . More precisely,  $\tau_2 \Delta E \sim n\hbar$ , where  $n$  is the value of the action in the decay and has the order of magnitude of the number of secondary particles. The case  $n = 1$  (decay into one  $\pi$  meson) occurs primarily at  $\omega_L \approx 200$  Mev (the so-called Tamm isobar<sup>13</sup>). However, here, too  $\tau_2 \gg \tau_1$ , but for other reasons due to the resonance character of the  $\pi N$  interaction in this energy region.

According to the sense of this method, one should insert in (3) the experimental cross section for the  $\pi N$  interaction instead of  $\sigma(\omega)$ . Hence, to calculate NN interactions of different types at 9 Bev, it is necessary to have the following data on the  $\pi N$  interaction in the energy region  $\omega_L \leq 2.5$  Bev:

a) The elastic and inelastic cross sections for the  $\pi N$  interaction and also the c.m.s. angular and momentum distributions of the secondary nucleons. These data were taken from experimental investigations.<sup>9-12\*</sup>

b) The multiplicity and prong distribution in inelastic  $\pi N$  interactions for the individual isospin states of the  $\pi N$  system. These data cannot be taken directly from the experiments. Since the experimental data are, as a rule, averaged over the isospin, we calculated these characteristics on the basis of the statistical theory.<sup>6-8</sup> It should be kept in mind here that in this energy region the statistical theory formulas for suitably chosen parameters are empirical formulas describing the experiment. Actually, all the calculations with formula (3) have to be performed numerically.

\*We note that the elastic  $\pi N$  interaction in the energy region 1 Bev  $< \omega_L < 2.5$  Bev is basically of a diffraction character.

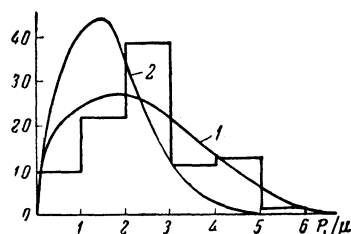


FIG. 2. Transverse momentum distribution of the nucleons (curves 1 and 2 are the theoretical curves for variants I and II, respectively; the histogram represents the experimental data<sup>1,2</sup>).

First, we calculated by formula (3) the total cross section  $\sigma_{NN}$ , which proved to be 18 mb. Here we imposed no additional restrictions on the value of the "virtualness"  $k^2$ . The basic contribution to the cross section came from cases with a virtualness not exceeding  $(7\mu)^2$ .

According to the experimental data, the cross section for the processes observed in references 1 and 2 was 21 mb. It thus follows that the pole approximation (if it is valid in the region  $k^2 \lesssim (7\mu)^2$ , can be used to describe a basic part of the experimental data. We therefore compared the results of the calculations with all the experimental material without an additional selection.

However, it was not clear beforehand whether the above assumptions were valid for large values of the quantity  $k^2 \sim (7\mu)^2$ . It was clear, however, that the smaller the value of  $k^2$ , the more justified were the assumptions. We therefore carried out the calculations with an additional restriction on the magnitude of the virtualness:  $k^2 \leq (3\mu)^2$ .\* [In this case, the term  $(\mu^2 + \kappa^2 + 4p_0P_1)^{-1}$  in formula (3) is replaced by an expression of the form  $(\delta^2 + \mu^2)^{-1}$ , where  $\delta^2 = k_{\max}^2 = (3\mu)^2$ .] In this variant, the cross section  $\sigma_{NN}$  turned out to be 4 mb. It thus follows that this variant can describe only a small part of the experimental data ( $\sim 20\%$ ); the results of the calculations in this case are valid only with a special selection of the experimental cases in which the value of the transferred momentum is small (these selection criteria are discussed below).

By carrying out the calculations for both variants and comparing them with the experiments, we hoped to obtain information on the applicability of the pole method in the region of  $k^2$  between  $(3\mu)^2$  and  $(7\mu)^2$ .

## RESULTS OF THE CALCULATIONS AND COMPARISON WITH EXPERIMENTAL DATA

1. The transverse momentum distribution of the nucleons ( $p_{\perp}$ ) is shown in Fig. 2 for the two methods of calculation: variant I with no restriction on  $k^2$  (curve 1) and variant II with  $k^2$

\*This variant already has been partially considered by Dremin and Chernavskii.<sup>4</sup>

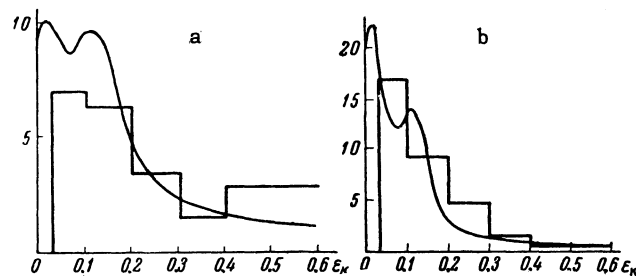


FIG. 3. Energy distribution of the recoil nucleons in the laboratory system: a – variant I, b – variant II; curves – theoretical results, histograms – experimental data (the kinetic energy of the recoil nucleons is laid off along the abscissa axis in fractions of the nucleon mass).

$\leq (3\mu)^2$  (curve 2). The experimental histogram is also shown in the figure. The curves and the histogram are normalized here (and below) to the same area. It is seen from the curves that in variant II practically all the nucleons have  $p_{\perp} \leq 2.5\mu$ ; the experimental distribution is significantly broader. Hence, to compare the experimental data with other characteristics obtained from the calculations by variant II, we selected from the former only those cases which satisfied the condition  $p_{\perp}^2 \leq 2.5$  (where  $p_{\perp}^2$  is the transverse momentum of the recoil proton).

Comparison of the experimental histogram with the curves obtained from variant I indicates satisfactory agreement. A difference (double the experimental error) occurs only in the interval  $p_{\perp} = 0 - 1\mu$ .

It should be noted that, in the theoretical calculation, the basic contribution in this region comes from cases in which two "ordinary" isobars with  $\mathfrak{M} = 1.3$  m and isospin  $3/2$  are produced, i.e., the isobars involved in the resonance scattering of 200-Mev  $\pi$  mesons.<sup>13</sup> On the other hand, there are grounds for assuming (see below) that a large number of these cases were missed in the experiments. This discrepancy can thus be attributed to "technical" rather than physical factors.

2. The energy distribution of the recoil nucleons is shown in Fig. 3a. Two facts are striking. First, the recoil nucleon spectrum drops sharply beginning with  $\epsilon_{\text{kin}} \sim 150$  Mev. This is characteristic for the picture of peripheral collisions and does not occur for "central" collisions. Second, the spectrum is not monotonic; a second weak maximum appears at  $\epsilon_{\text{kin}} = 120$ . This maximum is due to the contribution of cases in which one of the isobars has a mass  $\mathfrak{M} = 1.3$  m. Unfortunately, the experimental accuracy at the present time is insufficient for the separation of this maximum. It

**TABLE I.** C.m.s. angular distribution of nucleons. Calculations for pp collisions.

Cosine interval	Percentage of cases	
	variant I	variant II
1 —0,95	76	89,0
0,95—0,9	9	3,3
0,9 —0,85	4,2	3,2
0,85—0,8	3,9	2,5
0,8 —0,75	2,3	
0,75—0,7	1,4	
0,7 —0,6	2,3	
0,6 —0,5	2,2	2,0
0,5 —0,0	4,7	

is possible that it can be observed more easily at a higher nucleon energy.

Comparison of this curve with the experimental data indicates good agreement, except for the interval  $\epsilon_{\text{kin}} \leq 30$  Mev. However, in the experiment, cases in which the recoil nucleons had energies  $\epsilon_{\text{kin}} \leq 30$  Mev were simply discarded. On the other hand, according to the theoretical curve, about 10% of the cases are of this energy. It should be noted that the contribution to this region comes mainly from cases in which two isobars are produced with equal masses  $M_1 = M_2 = 1.3$  m.

An estimate (based on the statistical accuracy of the experiment) indicates that the "missing" of such cases is quite real. In this connection, it should be noted that the contribution of these cases to the transverse momentum curve may also have been "missed," as was already pointed out above.

The energy distribution of the recoil nucleons calculated by variant II is shown in Fig. 3b. Also shown there are the experimental data selected in accordance with the criterion  $p_{\perp}^T \leq 2.5 \mu$ . The agreement is good.

3. The c.m.s. angular distribution of the nucleons is shown in Table I. It is quite anisotropic

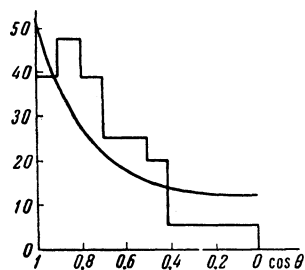


**FIG. 4.**  $\pi$ -meson c.m.s. angular distribution for variant I (pp interaction); the curves represent the theoretical results and the histogram represents the experimental data.<sup>1,2</sup>

both in variants I and II. The experimental data are not in contradiction with the calculations.

4. The  $\pi$ -meson angular distribution is shown in Fig. 4 along with the experimental histogram. It is seen that the  $\pi$ -meson angular distribution is anisotropic, although it is essentially wider than the nucleon angular distribution. The small difference in the low-angle region is apparently due to the same "technical" factors mentioned above. The difference in the large-angle region (the theoretical curve goes above the experimental points) may have a physical basis. On the whole, we consider the agreement to be satisfactory.

**TABLE II.** Multiplicity and prong distribution

Character of the star	Percentage of stars				
	Variant I			Variant II*	
	calc.	statistical theory	expt.	calc.	expt.
	pp interactions				
Two-prong	35	32,8	46±5,4	35	35±14
Four-prong	58,9	58,5	44,7±5,3	63,4	35±18
Six-prong	6,0	8,6	8,1±2,2	1,6	6±3
Eight-prong	0,1	0,1	0,62±0,62	—	—
Mean multiplicity	3,46	3,53	3,2	3,4	3,42
	pn interactions (variant I)				
One-prong	18,4	14,5	35,1±6,1		
Three-prong	65,2	59,4	53,2±7,5		
Five-prong	15,7	25,0	9,6±3,2		
Seven-prong	0,7	1,1	2,1±1,5		
Mean multiplicity	2,96	3,25	2,6		
Charged particle asymmetry	0,47	0	0,4±0,2		

\*The experimental data refer to cases in which the transverse momentum of the recoil proton is  $\leq 2.5 \mu$ . The theoretical calculations, in variant II took this into account.

5. We calculated the number of charged particles produced in  $\pi N$  interactions at energies  $\omega_L$  from 0.7 to 2 Bev by means of the statistical theory.\*

The probability for the production of the corresponding isobars was calculated on the basis of expression (3).

In variant I, we calculated the multiplicity and the prong distribution for pp and pn collisions. The results are shown in Table II, which lists also the experimental data and (for comparison) the results of the statistical theory calculations for

\*Here we took into account the contribution of the diffraction part of the interaction which constitutes  $\sim 30\%$  at an energy  $\omega_L > 1$  Bev. The determination of the number of "prongs" is in the latter case trivial. In the energy region  $\omega_L < 200$  Mev, where the interaction is elastic, the number of prongs was found from considerations of charge symmetry.

central NN collisions under the assumption of the production of a single system of mass:  $M = 5$  Bev.

Attention is drawn to the fact, first, that the calculated multiplicity in peripheral collisions was found to be of the same order as in central collisions. The reason for this is that the multiplicity is a weak function of the energy, and the production of two "isobars" of smaller mass can give the same multiplicity as the production of one "compound" system of large mass. Second, the other enumerated characteristics (for example, the c.m.s. asymmetry of the charge distribution) listed in Table II are essentially different from the results of the statistical theory calculations for "central" collisions (in general, no asymmetry can occur there).

The experimental data do not contradict the obtained values (within the limits of two times the error), but it cannot be stated that there is full agreement. The calculated multiplicity is somewhat greater than the observed one, but the calculated charge asymmetry is in agreement with that observed.

In variant II, the calculations were performed only for pp interactions under an additional condition: we selected only cases in which a proton was emitted "backward" in the c.m.s. The results of these calculations are shown in Table II along with the experimental data selected in accordance with the criterion  $p_{\perp}^F \leq 2.5 \mu$ . The agreement is good.

## CONCLUSIONS

The comparison of the theoretical results with experiment indicates that the peripheral one-meson interaction calculated by the pole method satisfactorily describes the basic part of the experimental data, and, consequently, the pole approximation is applicable in the region  $k^2 \lesssim (7\mu)^2$  important to the calculations.\* This can serve as an indication that, first, the nonpole term in the propagation function (1) is small in the region  $k^2 \lesssim (7\mu)^2$  in comparison with the pole term, and, second, the cross section is a smooth, slowly-varying function of  $k^2$  up to  $k^2 \sim (7\mu)^2$  [This, of course, does not exclude the possibility that the nonpole terms in (1) and (2) are both large, but in the region  $k^2 \leq (7\mu)^2$  they offset one another.]

The marked difference between the calculations and experiment as regards the multiplicity indi-

cates that the role of the second term in (2) is more important than the second term in (1). Indeed, if we allow for the drop in the cross section with an increase in  $k^2$ , we could reduce the role of the cases of high multiplicity in the calculation and bring about agreement with experiment; the inclusion of the second term in the propagation function can only increase the multiplicity.

Hence it seems that such experiments and the improvement of their accuracy can provide information (although indirectly) on very important quantities in contemporary theoretical physics, the functions  $\rho(k)$  and  $\sigma(k^2)$ . This is of interest, since thus far there are no other experimental sources of such information. The fact that the results of the calculations by the second variant [ $k^2 \leq (3\mu)^2$ ] are in good agreement with part of the experimental stars (selected in accordance with the criterion  $p_{\perp} \leq 2.5 \mu$ ) is important in this situation only as an additional confirmation; they do not give any new information.

Comparison of the absolute values of the cross sections indicates that the contribution of interactions of another type (for example, multi-meson, K-meson, central, etc.) can constitute 20 — 30% of the total cross section. However, it is not possible to separate them by their total mass in a given experiment, since it is difficult, at present, to indicate criteria for such a separation.\*

In conclusion, the authors take this opportunity to express their gratitude to E. L. Feinberg and V. I. Veksler for their constant interest in this work and valuable comments.

<sup>1</sup>Bogachev, Bunyatov, Gramenitskii, Lyubimov, Merekov, Podgoretskii, Sidorov, and Tuvdendorzh, JETP 37, 1225 (1959), Soviet Phys. JETP 10, 872 (1960).

<sup>2</sup>Wang Shu-Fen, Visky, Gramenitskii, Grishin, Lebedev, Dalkhazhav, Nomofilov, Podgoretskii, and Strel'tsov, JETP 39, 957 (1960), Soviet Phys. JETP 12, 663 (1961).

<sup>3</sup>G. F. Chew and F. E. Low, Phys. Rev. 113, 1640 (1959).

<sup>4</sup>I. M. Dremin and D. S. Chernavskii, JETP 38, 229 (1960), Soviet Phys. JETP 11, 167 (1960).

<sup>5</sup>V. B. Berestetskii and I. Ya. Pomeranchuk, JETP 39, 1078 (1960), Soviet Phys. JETP 12, 752 (1961).

<sup>6</sup>E. Fermi, Progr. Theoret. Phys. (Kyoto) 5, 570 (1950); Phys. Rev. 81, 683 (1951).

\*A similar calculation and comparison with the experimental data at 200 Bev<sup>14,15</sup> gives additional information on the character of the pole approximation at larger  $k^2$ . This question has been considered separately.<sup>16</sup>

\*A large multiplicity in a star (as was explained above) cannot serve as such a criterion.

<sup>7</sup>S. Z. Belen'kii and L. D. Landau, Usp. Fiz. Nauk **56**, 309 (1955).

<sup>8</sup>Belen'kii, Maksimenko, Nikishov, and Rozental', Usp. Fiz. Nauk **62**, No. 2, 1 (1957).

<sup>9</sup>H. Bethe and F. de Hoffman, Mesons and Fields, Row, Peterson and Co., New York, 1955, vol. 2.

<sup>10</sup>Burrowes, Caldwell, Frisch, Hill, Ritson, Schluter, and Wahlig, Phys. Rev. Lett. **2**, 119 (1959).

<sup>11</sup>Chretien, Leitner, Samios, Schwartz, and Steinberger, Phys. Rev. **108**, 383 (1957).

<sup>12</sup>R. C. Whitten and M. M. Block, Phys. Rev. **111**, 1675 (1958).

<sup>13</sup>Tamm, Gol'fand, and Faïnberg, JETP **26**, 649 (1954).

<sup>14</sup>S. A. Slavatinskii, Moscow Cosmic Ray Conf. 1959.

<sup>15</sup>N. A. Dobrotin, 1960 Annual Intern. Conf. on High Energy Physics at Rochester.

<sup>16</sup>I. M. Dremin and D. S. Chernavskii, JETP (in press).

Translated by E. Marquit  
182